

Acute and late-onset optic atrophy due to a novel OPA1 mutation leading to a mitochondrial coupling defect

Yannick Nochez,¹ Sophie Arsene,¹ Naig Gueguen,^{2,3} Arnaud Chevrollier,^{2,3} Marc Ferré,^{2,3,4} Virginie Guillet,^{3,4} Valérie Desquret,² Annick Toutain,⁵ Dominique Bonneau,^{2,3,4} Vincent Procaccio,^{2,4,6,7} Patrizia Amati-Bonneau,^{2,3} Pierre-Jean Pisella,¹ Pascal Reynier^{2,3,4}

¹Centre Hospitalier Universitaire de Tours, Service d'Ophtalmologie, Tours, France; ²CHU d'Angers, Département de Biochimie et Génétique, Angers, France; ³INSERM, U694, Angers, France; ⁴Université d'Angers, Faculté de Médecine, Angers, France; ⁵Centre Hospitalier Universitaire de Tours, Service de Génétique, Tours, France; ⁶CNRS, UMR6214, Angers, France; ⁷INSERM, U771, Angers, France

Purpose: Autosomal dominant optic atrophy (ADOA, OMIM 165500), an inherited optic neuropathy that leads to retinal ganglion cell degeneration and reduced visual acuity during the early decades of life, is mainly associated with mutations in the *OPA1* gene. Here we report a novel ADOA phenotype associated with a new pathogenic *OPA1* gene mutation.

Methods: The patient, a 62-year-old woman, was referred for acute, painless, and severe visual loss in her right eye. Acute visual loss in her left eye occurred a year after initial presentation. MRI confirmed the diagnosis of isolated atrophic bilateral optic neuropathy. We performed DNA sequencing of the entire coding sequence and the exon/intron junctions of the *OPA1* gene, and we searched for the mitochondrial DNA mutations responsible for Leber hereditary optic atrophy by sequencing entirely mitochondrial DNA. Mitochondrial respiratory chain complex activity and mitochondrial morphology were investigated in skin fibroblasts from the patient and controls.

Results: We identified a novel heterozygous missense mutation (c.2794C>T) in exon 27 of the *OPA1* gene, resulting in an amino acid change (p.R932C) in the protein. This mutation, which affects a highly conserved amino acids, has not been previously reported, and was absent in 400 control chromosomes. Mitochondrial DNA sequence analysis did not reveal any mutation associated with Leber hereditary optic neuropathy or any pathogenic mutations. The investigation of skin fibroblasts from the patient revealed a coupling defect of oxidative phosphorylation and a larger proportion of short mitochondria than in controls.

Conclusions: The presence of an *OPA1* mutation indicates that this sporadic, late-onset acute case of optic neuropathy is related to ADOA and to a mitochondrial energetic defect. This suggests that the mutational screening of the *OPA1* gene would be justified in atypical cases of optic nerve atrophy with no evident cause.

Autosomal dominant optic atrophy (ADOA, OMIM 165500) is a hereditary disorder characterized by progressive loss of visual acuity in the early decades of life, color vision deficits, optic nerve pallor, and central or centrocecal visual field scotoma [1,2]. ADOA occurs with an estimated prevalence of 1:50,000 in most populations [3], and 1:10,000 in Denmark [4]. This hereditary optic neuropathy leads to phenotypic heterogeneity, even among members of a given family [5]. Histopathological studies indicate that ADOA is caused by the degeneration of retinal ganglion cells followed by the ascending atrophy of the optic nerve [6].

In 2000, two research groups identified *OPA1* gene mutations on chromosome 3q28 as causing ADOA [7,8]. The *OPA1* gene encodes a dynamin-related guanosine triphosphatase (GTPase) and is composed of 31 exons [9]. As of January 2009, 204 *OPA1* pathogenic mutations have been

reported, mainly in the GTPase and the C-terminal domains of the protein (eOPA1) [10]. The *OPA1* protein is localized to the mitochondrial intermembrane space, where it facilitates fusion between mitochondria [11]. The protein is involved in several mitochondrial functions, such as the maintenance of the integrity of the cristae formed by the mitochondrial inner membrane [12], the regulation of cytochrome c release during apoptosis [13], and the maintenance of mitochondrial DNA [14,15].

Studies of patients carrying pathogenic *OPA1* mutations have revealed the great diversity of clinical presentations of ADOA by the description of congenital forms of the disease [16], of forms with spontaneous visual recovery [17], and forms associated with extraocular symptoms such as deafness [18], polyneuropathy [19], chronic progressive ophthalmoplegia [20], myopathy, and encephalopathy [14, 15]. An energy impairment has been found to be associated with the disease in vivo [21] as well as in the patient's fibroblasts [22]. In addition to this energy impairment, it has been shown that the mitochondrial network of mutated fibroblasts was frequently fragmented and that some *OPA1*

Correspondence to: Dr. Yannick Nochez, Service d'Ophtalmologie, CHRU de Tours, 2 Boulevard Tonnellé, F-37000, Tours, France; Phone: +33 2 47 47 87 66; FAX: +33 2 47 47 80 61; email: yannick.nochez@free.fr

mutations were associated to increased susceptibility to apoptosis [23]. Lastly, patients with severe ADOA with extraocular symptom were found to harbor multiple mitochondrial DNA deletions [14,15], reinforcing the strong links existing between mitochondrial structure maintenance and mitochondrial energetic metabolism in neurodegenerative diseases.

The aim of the present report is to show that a clinical phenotype similar to that of late-onset Leber hereditary optic neuropathy may be linked to an OPA1 mutation. This report, together with other recent studies, reveals the unexpected clinical heterogeneity of ADOA caused by OPA1 mutations.

METHODS

Patient history: A 62-year-old Caucasian woman consulted for blurred vision. On examination, she was found to have a central scotoma in the right eye; visual failure occurred rapidly a few days later. She denied having had any previous ocular symptoms, ocular pain, or systemic symptoms such as headache, muscular pain, or jaw claudication. An ophthalmic examination documented a right optic disc edema without peripapillary hemorrhage. No morphological abnormalities in optic disc cupping or loss of the neuroretinal rim were found in either eye. The visual acuity in the right eye, which had a large central scotoma, fell to 20/400, but remained at 20/20 in the left eye. The intraocular pressure in each eye was 15 mmHg.

The patient had no known vascular risk factors. She showed no signs of hypertension, diabetes, or hyperlipidemia, and did not indulge in alcohol or tobacco. The electrocardiogram was normal, without any signs of dysrhythmia. The carotid and the transcranial Doppler scans showed no prominent stenosis or occlusion of the major intracranial large arteries. The general and neurologic examinations were normal. Brain MRI was normal. Laboratory investigations were done to exclude other causes of arteritis, such as syphilis, hepatitis, Lyme disease, or systemic lupus erythromatosis. The erythrocyte sedimentation rate and the C-reactive protein level were not elevated. A temporal artery biopsy, done to check for inflammatory arterial cells, was normal. As the patient was suspected of having giant-cell arteritis and arteritic anterior ischemic optic neuropathy, she was treated with 500 mg I.V. methylprednisolone for three days, while awaiting biopsy results, to prevent vision loss from progressing to the other eye. Visual acuity remained 20/400 in the right eye, with resolution of the disc edema.

Nine months after the loss of vision in the right eye, vision in the left eye became blurred and worsened to 20/250 over the following week. On ophthalmoscopic examination, the left optic disc showed edema without splinter hemorrhages at the disc margin. The swelling of the optic disc gradually subsided and turned pale. The same clinical, biologic, and

radiological investigations as before showed no abnormalities. Brain and orbital MRI was normal. Our hypothesis was that the patient had an acute anterior ischemic optic neuropathy, caused either by an inflammatory involvement of the optic nerve or by an ischemic sequela to vasculitis. Since there may have been some overlap between the two conditions, the patient was treated with intravenous methylprednisolone to try to improve her vision. Nevertheless, the visual acuity remained at 20/250 in the left eye, with resolution of the disc edema.

At the last examination six months later, the patient, still amaurotic, was given a poor prognosis for further recovery of the visual defects. Fundus examination revealed severe optic disc atrophy in both eyes (Figure 1). The clinical examination and the MRI confirmed the diagnosis of isolated bilateral optic neuropathy. We searched for a genetic etiology. The patient's parents were dead; she had no brothers or sisters; but she had a 28-year-old son who had no ophthalmic problems.

OPA1 gene analysis: Blood samples were taken from the patient after obtaining informed consent. Genomic DNA was extracted from blood samples using the BioRobot EZ1 and the EZ1 DNA Blood kit (Qiagen, Courtaboeuf, France). Next, 30 primer pairs (Appendix 1) were used to amplify the 30 OPA1 coding exons, including exon-intron junctions. PCR amplifications of the DNA were conducted under standard protocols. The purified PCR products were sequenced using a Ceq2000 DNA sequencer (CEQ DTCS-Quick Start kit; Beckman Coulter, Fullerton, CA). The OPA1 mutation is described according to the OPA1 transcript variant 1 (RefSeq: [NM_015560](#)).

Mitochondrial DNA analysis: To exclude the presence of any rare mitochondrial DNA mutation, we sequenced entirely the mitochondrial genome. The mtDNA was PCR amplified in eight fragments using the protocol 96 °C for 10 min, followed by 30 cycles of 96 °C for 45 s, 58 °C for 30 s, 72 °C for 3 min, and a last extension at 72 °C for 10 min (Appendix 2). PCR products were purified and sequenced as described in the previous section.

Skin fibroblasts: The research followed the tenets of the Declaration of Helsinki. Fibroblast cells were obtained from skin biopsies taken after obtaining written consent from the patient, as described elsewhere [24]. Fibroblasts, obtained by explants from skin punch biopsy, were maintained in DMEM (Invitrogen, Carlsbad, CA) with 10% bovine calf serum at 37 °C in a humidified atmosphere with 5% CO₂. All fibroblast cultures were mycoplasma-free, as shown by the DAPI/Hoechst in situ coloration and by PCR (Venor®Gem, BioValley, Marne-la-Vallée, France). All experiments were performed on cells with similar passage numbers, ranging from 5 to 15, so as to avoid artifacts due to senescence, known to occur at passage numbers greater than 30.

Efficiency of mitochondrial ATP production in permeabilized cells: The rate of mitochondrial ATP synthesis and the ATP/

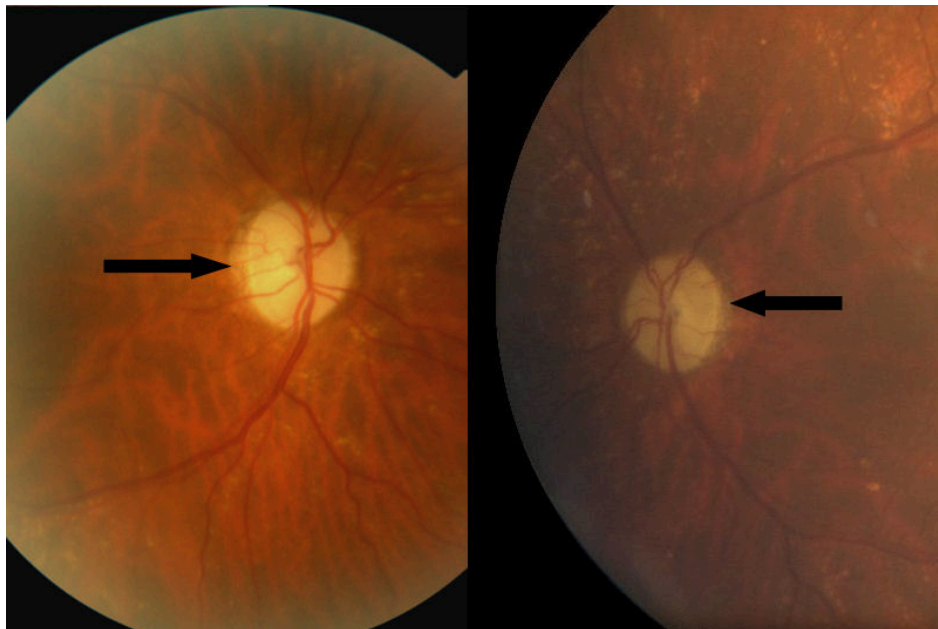


Figure 1. Fundus examination. The first image represents the patient's right eye fundus examination and we observe optic disk atrophy (arrow). The second image represents left eye fundus examination, we also observe optic disk atrophy.

O ratio were determined in cells permeabilized by exposure to digitonin, as described below [24]. Cells were resuspended in the respiratory buffer, which contained 10 mM KH_2PO_4 , 300 mM mannitol, 10 mM KCl, and 5 mM MgCl_2 , pH 7.4. This buffer was supplemented with 2 mM iodoacetate and 2 mM EDTA so as to prevent glycolytic ATP synthesis and ATP hydrolysis by cellular ATPases. The respiratory rates ($\text{O}_2/\text{min}/\text{mg}$ of proteins) of $3\text{--}5 \times 10^6$ cells were recorded at 37°C in 2 ml glass chambers using a two-channel, high-resolution Oxygraph respirometer (Oroboros, Innsbruck, Austria). ATP synthesis was started by addition of 5 mM malate, 5 mM pyruvate, and 10 mM succinate, followed by addition of 1.5 mM ADP. Five aliquots were sampled each minute during mitochondrial ATP synthesis, quenched with an equal volume of 1% (W/V) TCA solution and neutralized by adding a 25 mM HEPES, 2 mM EDTA, pH 7.75 buffer. Three aliquots were also sampled after addition of 8 $\mu\text{g}/\text{ml}$ oligomycin (an ATP synthase inhibitor) to check for residual nonmitochondrial ATP synthesis. The ATP synthesized in situ was measured using the Enliten ATP assay (Promega, Madison, WI). Luminescence was measured on a multidetection reader for microplates Xenius XML (SAFAS, Monaco, Monaco) using a 10-s integration period. Standardization was performed with known quantities of ATP measured under the same conditions. Coupling efficiency (ATP/oxygen [ATP/O]) was measured by polarography as the number of nanomoles of ATP produced from ADP+Pi per nanomole of oxygen consumed by permeabilized cells. The efficiency of the respiratory chain was tested using malate, pyruvate, and succinate as substrates.

A Beckman DU 640 spectrophotometer (Beckman Coulter, Fullerton, CA) was used to measure the activity of

the mitochondrial respiratory chain complexes on cell homogenates at 37°C in a cell buffer that contained 250 mM saccharose, 20 mM tris[hydroxymethyl]aminomethane, 2 mM EGTA, and 1 mg/ml BSA, pH 7.2. Complex IV (cytochrome c oxidase, COX), complex V (F1-ATPase), and citrate synthase activities were recorded following Rustin et al. [25]. Complex IV activity was measured in a 50 mM KH_2PO_4 buffer, using 15 μM reduced cytochrome *c* on 10^5 cells permeabilized by 2.5 mM $\beta\text{-D-dodecylmaltoside}$. To measure the activity of complex V, we first disrupted cells by freezing in liquid nitrogen, followed by rapid thawing at 37°C . The cells were then centrifuged for 2 min at $800 \times g$, resuspended in cell buffer (250 $\mu\text{l}/10^6$ cells). This was followed by a sonication step (6 \times 5 s with an MSE sonicator). Complex V activity was immediately assayed on this cell lysate (0.5×10^6 cells) in a Tris/KCl buffer, composed of 50 mM Tris and 10 mM KCl, and containing 2 mM Phosphoenolpyruvate (PEP), 0.5 mM ATP, 5 mM MgCl_2 , 1.5 μM FCCP, 2.5 $\mu\text{g}/\mu\text{l}$ antimycin A, 0.1 U lactate dehydrogenase, and 0.1 U pyruvate kinase (Roche Diagnostics, Meylan, France), 5 mg/ml BSA, pH 8. After incubation for 3 min, the reaction was started by adding 0.1 mM NADH and the rate of disappearance of NADH was monitored at 340 nm. In addition, 10 μM oligomycin was added to determine the background rate (nonspecific for complex V activity). Citrate synthase was assayed by standard procedures, using 0.15 mM 5-5-dithiobis(2-nitrobenzoic acid) (DTNB), 0.5 mM oxaloacetate, 0.3 mM acetyl-CoA, and 0.1% (V/V) Triton X-100. Specific enzymatic activities were expressed in mIU (e.g., nanomoles of cytochrome *c*, NADH or DTNB/min/mg protein, respectively). Enzymatic activities of complexes IV, V and citrate synthase are listed in Table 1.

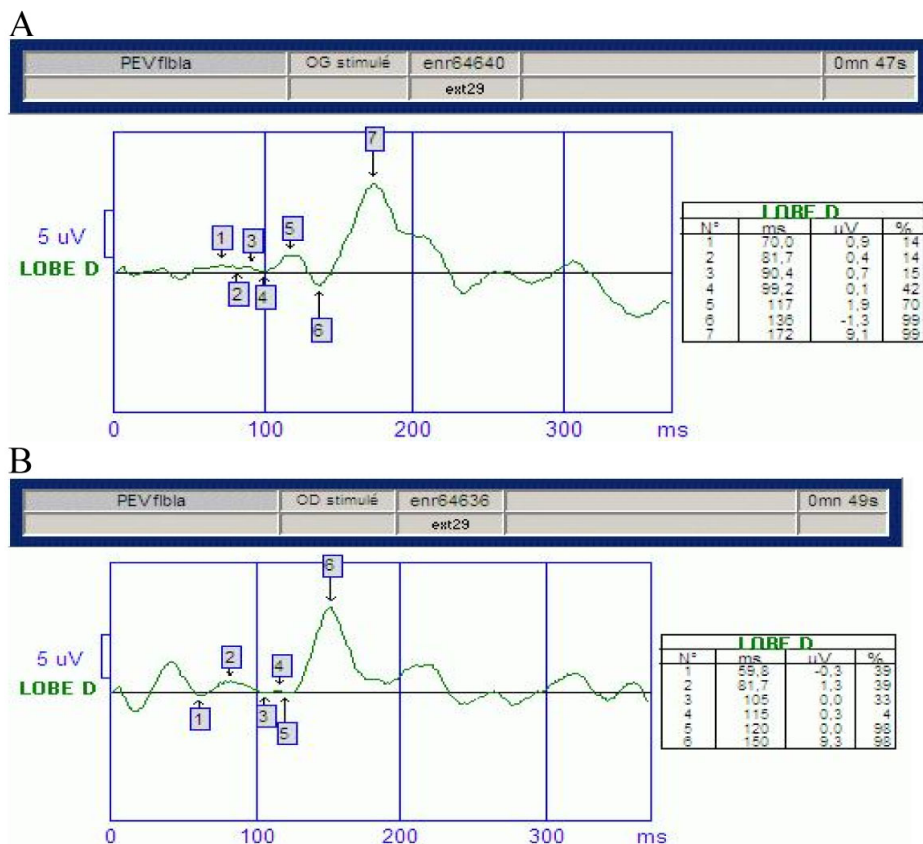


Figure 2. Patient 's visual evoked potentials. We observe low-amplitude potentials and increased latency in visual evoked potentials in left eye (A) and in right eye (B). It indicates defective conduction of the optic nerves.

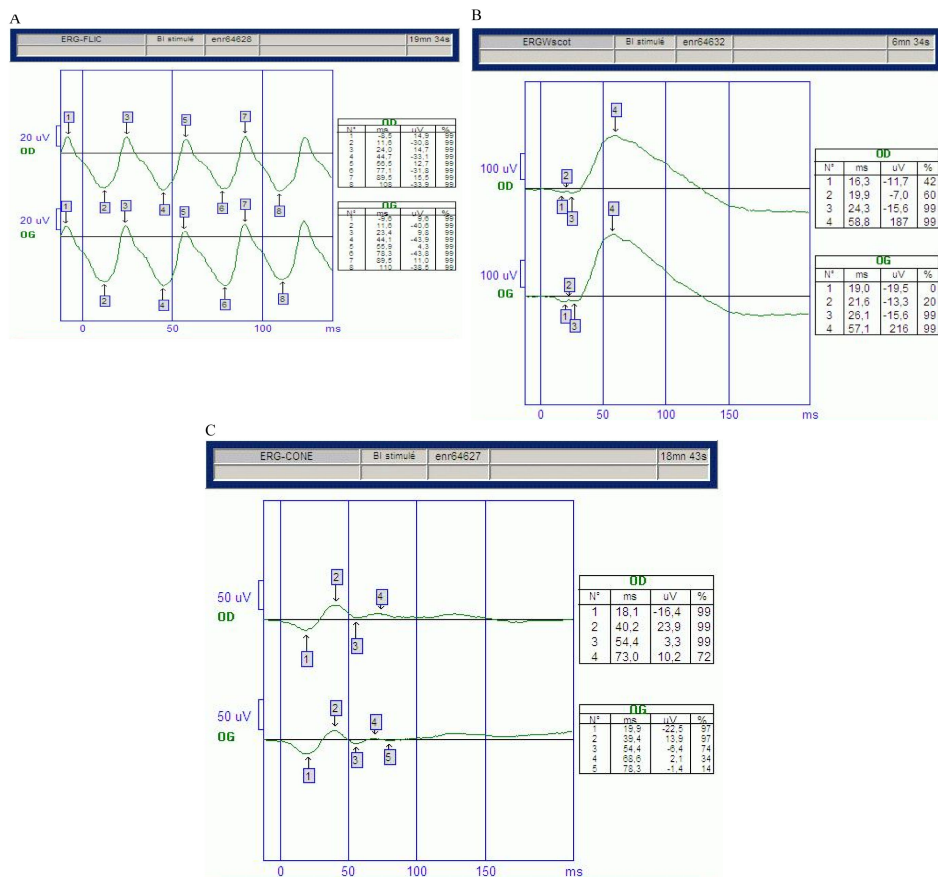
Mitochondrial fluorescence imaging: Cells cultured in a two-well chamber slide (Labtek, Nunc International, Naperville, IL) were incubated with 100 nM Mitotracker® to label the mitochondrial network (Molecular Probes, Carlsbad, CA) according to manufacturer's instructions. Z-Stack fluorescent images were acquired with a Leica (DMI6000B; Microsystems GmbH, Wetzlar, Germany) and a Roper CoolSnap HQ2 camera. MetaMorph software (Molecular Devices, Sunnyvale, CA) was used to analyze images. Mitochondrial length and number were determined using integrated morphometric analysis of the regions created around mitochondria after deconvolution (MetaMorph®, Molecular Devices), as described above by Cassereau et al. [26]. Around 50 deconvolved images were used to quantify the mitochondrial length. Measurements of mitochondria length distribution were divided into four groups: <1 μm, 1 to 5 μm, 5 to 10 μm, and >10 μm.

Expression of OPA1 protein: Pellets of 5×10^6 fibroblasts from the patient and controls were stored at -80°C until used for western blot analysis. Next, 40 μg protein were solubilized in Laemmli buffer and heated for 5 min at 50°C . Proteins were separated on an 8% SDS-polyacrylamide gel and electroblotted to a PVDF membrane (Amersham Biosciences, Buckinghamshire, UK). Membranes were saturated overnight at 4°C with 5% nonfat milk dissolved in TBS-Tween-0.1%,

pH 7.4, which contained 137 mM NaCl, 2.7 mM KCl, 23 mM Tris, and 0.1% Tween-20. Membranes were then incubated 2 h at room temperature with monoclonal mouse anti-OPA1 antibody (BD Bioscience PharMingen, Milan, Italy) and mouse monoclonal anti-Hsp60 antibody (Stressgene, Victoria, Canada). Membranes were then washed three times in TBS-Tween-0.1% and incubated with 1:10,000 horseradish peroxidase-conjugated rabbit anti-mouse secondary antibody for 1 h at room temperature. The immunoreactive proteins were visualized with enhanced chemiluminescence (ECL Plus Western Blotting Detection Reagents; Amersham Biosciences). Band intensities were quantified with Quantity One software (Bio-Rad, Hercules, CA).

RESULTS

The clinical examination and MRI confirmed the diagnosis of isolated bilateral optic neuropathy in our patient. Visual fields showed large centrocecal defects and central visual field loss. Visual evoked potential to a bright flash showed low-amplitude potentials and increased latency in both eyes, indicating defective conduction of the optic nerves (Figure 2). Flash-electroretinograms and flicker electroretinograms were within normal limits (Figure 3). Color-axis confusion lines were not specific because of many mistakes due to low visual acuity. MRI of the optic nerve showed severe bilateral atrophy



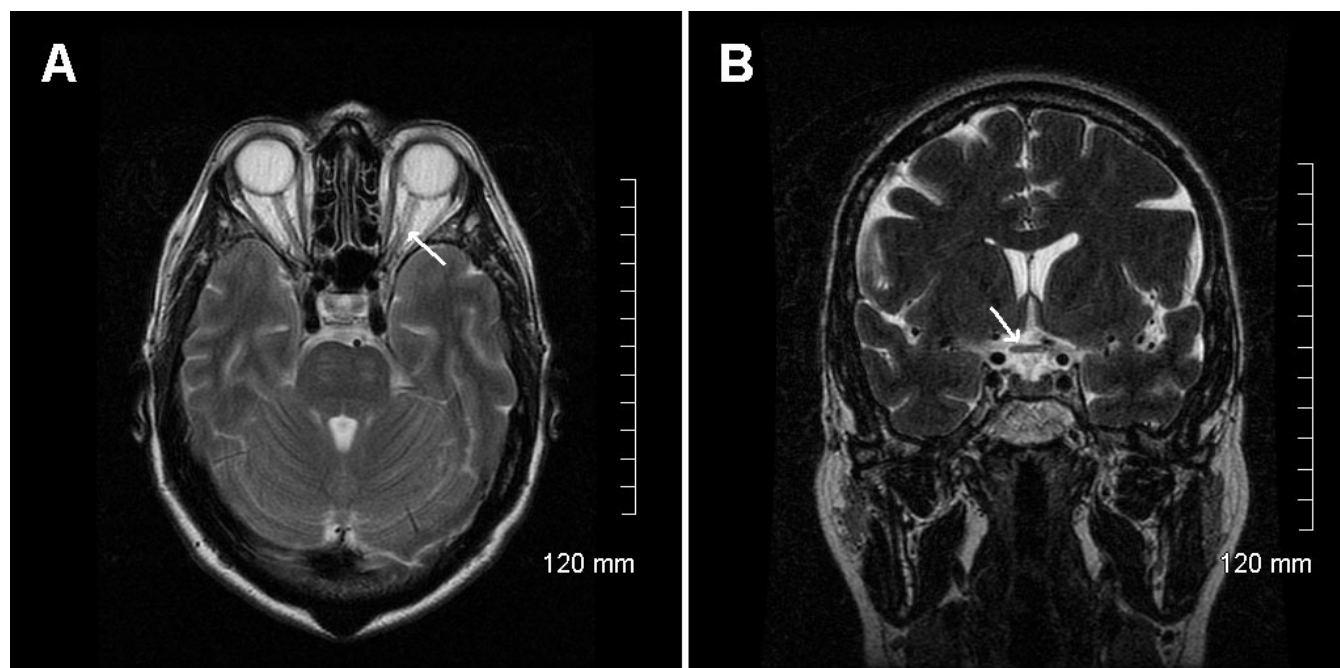


Figure 4. Patient's encephalic MRI. MRI of the optic nerve showed severe bilateral atrophy of the optic nerve from retina to the lateral geniculate nucleus, seen on horizontal MRI section (A), including atrophy of the optic chiasma, seen on coronal MRI section (B).

TABLE 1. ENZYMATIC ACTIVITIES OF COMPLEXES IV, V AND CITRATE SYNTHASE.

Cells	Complex IV	Complex V	CS	Complex IV/CS	Complex V/CS
controls	256±40	123±31	362±75	0.68±0.12	0.38±0.11
ADOA	185±44	214±52	363±65	0.51±0.08	0.62±0.15
OPA1_R932C	105	200	368	0.29	0.54

The enzymatic activities were measured in three experiments for the patient and each control subject (n=6). Results are expressed as mIU (nmol substrate/min/mg protein), and normalized to citrate synthase. Results are given as mean±standard deviation.

observed in fibroblasts from patient with OPA1 mutations. However, this observation is not correlated to a fragmented network, which could be shown in apoptotic cells. Culture cell studies performed on patient's cells did not show a higher rate of apoptosis nor a greater number of necrotic cells as compared to controls. These results were obtained using a viability test (Trypan blue exclusion test, data not shown).

In spite of the mutation, there was no quantitative modification of OPA1 expression in the patient's fibroblasts. We also observed no alteration of the OPA1 expression pattern in these cells (Figure 7).

DISCUSSION

ADOA is an inherited optic neuropathy that leads to reduced visual acuity. It is classically characterized by the insidious onset of visual impairment in early childhood with moderate to severe loss of visual acuity, temporal optic disc pallor, color vision deficits, and centrocecal scotoma of variable density [28]. Histopathologic studies have shown that the fundamental underlying defect is degeneration of the retinal ganglion cells, followed by ascending optic atrophy [1]. In about 70% of the cases, ADOA is due to mutations in the

nuclear *OPA1* gene situated on chromosome 3q28-q29 [7,8, 29]. The OPA1 protein is a dynamin-related GTPase targeted to mitochondria, where it is anchored to the mitochondrial inner membrane [11,30]. Our analysis of the mitochondrial network showed that fibroblasts with the c.2794C>T mutation contained a larger proportion of short mitochondria than controls (Figure 6). This finding is in accordance with the functional involvement of OPA1 in the structure of the mitochondrial network and with the alterations of mitochondrial structure observed in fibroblasts carrying OPA1 mutations [23].

Since the first description of the disease [6], the classic presentation of ADOA has widened to include less typical features. Indeed, gender-related variations and intrafamilial phenotypes heterogeneity of ADOA have been reported [31]. Visual loss has been found to be more severe in affected males than in females [31]. The expression of the disease is highly variable, even within a given family, and asymptomatic carriers can be found in some families [5,32]. The availability of molecular testing has revealed phenotypic variations, such as severe congenital forms of optic atrophy [16], ADOA associated with sensorineural deafness [18], and ADOA

TABLE 2. SEQUENCE VARIATIONS OF THE PATIENT'S MITOCHONDRIAL GENOME.

Nucleotide position	Amino acid substitution	Locus	Presence in Mitomap database	Status
m.263A>G	-	MT-DLOOP	Yes	Polymorphism
m.310_311insC	-	MT-DLOOP	Yes	Polymorphism
m.750A>G	-	MT-RNR1	Yes	Polymorphism
m.1438A>G	-	MT-RNR1	Yes	Polymorphism
m.2363A>G	-	MT-RNR2	No	Unknown
m.3010G>A	-	MT-RNR2	Yes	Polymorphism
m.4769A>G	p.M100M	MT-ND2	Yes	Synonymous change
m.8860A>G	p.T112A	MT-ATP6	Yes	Polymorphism
m.9966G>A	p.V254I	MT-CO3	Yes	Polymorphism
m.15326A>G	p.T194A	MT-CYB	Yes	Polymorphism
m.15742C>A	p.L332L	MT-CYB	No	Synonymous change
m.16092T>C	-	MT-DLOOP	Yes	Polymorphism
m.16297T>C	-	MT-DLOOP	Yes	Polymorphism
m.16519T>C	-	MT-DLOOP	Yes	Polymorphism

The patient's mtDNA was entirely sequenced. The sequence was compared to the revised Cambridge reference sequence of Human mtDNA. The patient was found to carry 14 nucleotide variations. No known or potential pathogenic mtDNA mutation were identified.

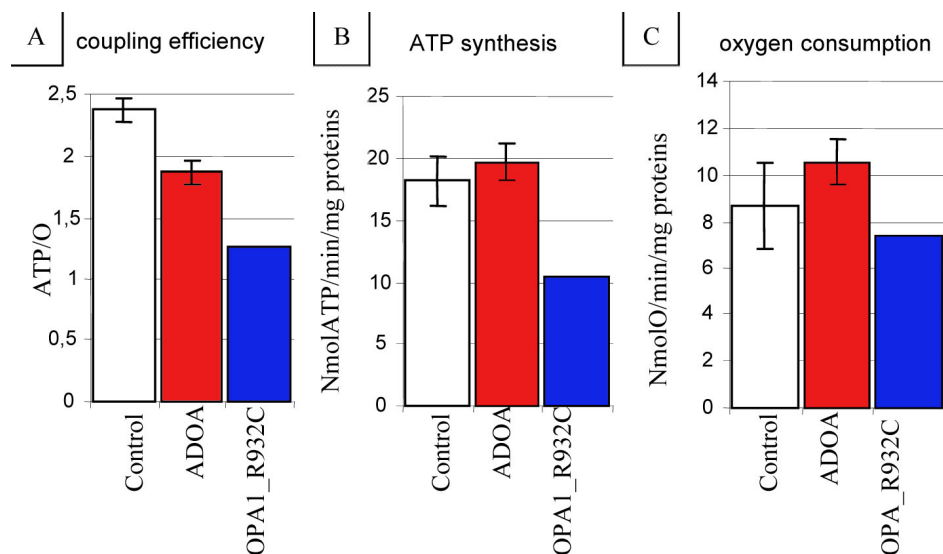


Figure 5. Mitochondrial metabolic investigations in the patient and controls. **A:** Coupling efficiency (ATP/O): Reduced efficiency of ATP synthesis was found in the patient's fibroblasts in comparison to controls. **B:** Reduced mitochondrial ATP synthesis, measured by luminescence from aliquot samples in a polarographic chamber, was found in the patient's fibroblasts in comparison to controls. **C:** Maximal coupled respiration rates, i.e., ADP-stimulated oxygen consumption with malate, pyruvate, and succinate, was measured in the same polarographic chamber.

associated with more complex, severe multi-organ phenotypes [14,15]. However, no correlation has been found between the degree of visual impairment and the location or type of mutation in *OPA1* [33,34]. The cause of this variable phenotypic expression remains to be elucidated but could be due to various genetic or environmental factors. Other genes encoding proteins involved in the modulation of mitochondrial bioenergetics and structure may influence the phenotypic expression of the disease. For instance it has been shown that the mitochondrial DNA, which encodes respiratory chain subunits, can influence the expression of ADOA [35]. Environmental factors such as drugs with

mitochondrial toxicity could also be involved in the penetrance and expressivity of the disease.

Our case report demonstrates the existence of a new mode of onset of ADOA related to *OPA1* mutation with an acute and a late onset that contrast with the earlier and insidious onset of the disease classically observed and described. The acute-onset presentation of optic atrophies is usually associated with Leber hereditary optic neuropathy, which remains the main differential diagnosis of ADOA. This mitochondrial DNA mutation-related disease is classically associated with acute or subacute bilateral optic atrophy occurring in the third decade of life, and preferentially affecting males [36]. Our observation shows that acute-onset

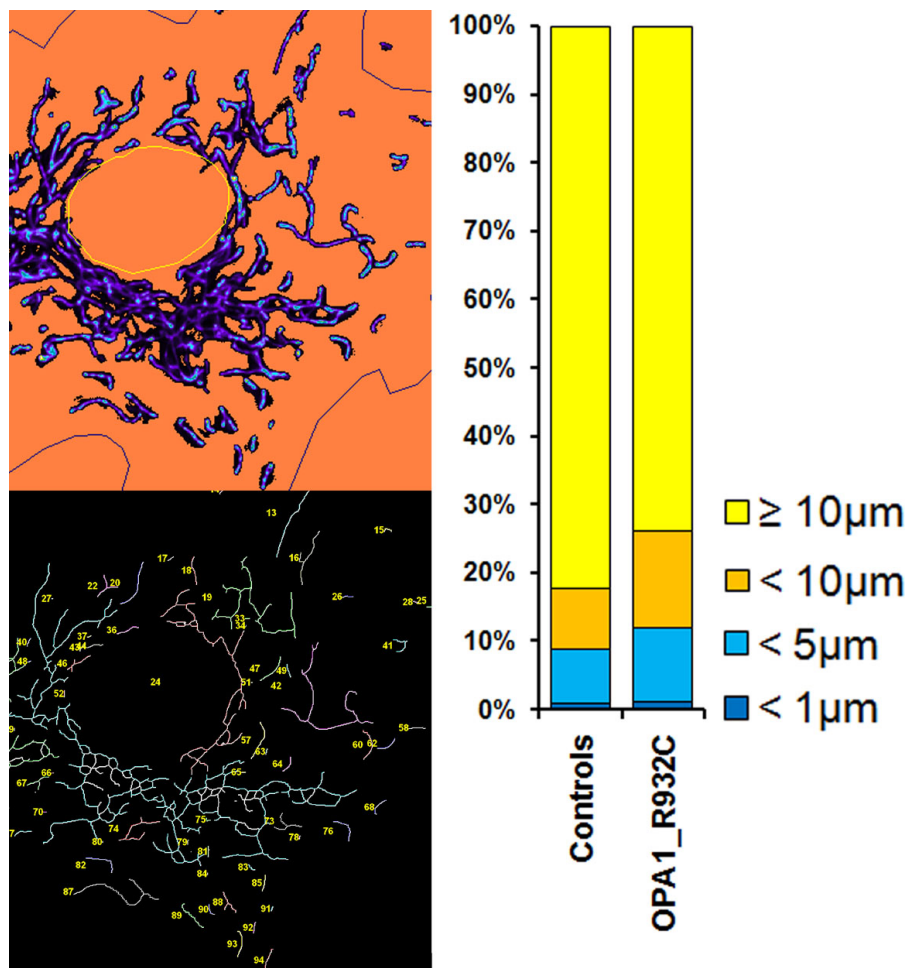


Figure 6. Quantification of mitochondrial shape showed that the patient's fibroblasts (OPA1_R932C) contained a higher proportion of short mitochondria than controls (Appendix 3).

presentations should benefit from *OPA1* analysis when LHON mutations have been excluded. Late-onset cases of optic atrophies are rarely considered to be caused by primary hereditary diseases but frequently believed to be due to secondary causes. Our case shows that *OPA1* analysis can be useful in late-onset cases of ADOA when the main secondary causes of optic atrophies have been excluded.

The novel *OPA1* mutation is associated with a mitochondrial energy defect involving reduced ATP synthesis and a cytochrome c oxidase deficiency. A similar, but less marked, biochemical phenotype has been previously described in fibroblasts from patients with ADOA carrying *OPA1* mutations; in this study the reduced efficiency of oxidative phosphorylation was found to be compensated by a higher rate of mitochondrial respiration to maintain ATP synthesis [22]. In our case, the marked decrease in COX activity might limit the possibility of compensation by a higher rate of mitochondrial respiration.

In conclusion, we report a novel *OPA1* mutation in a patient with ADOA characterized by sporadic, acute, and late-

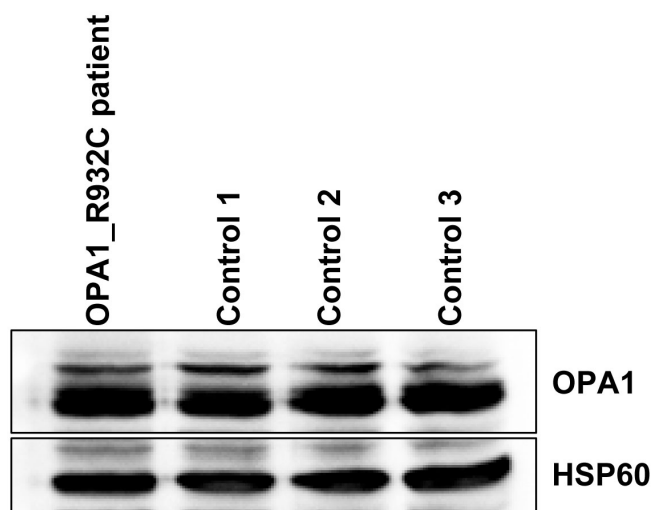


Figure 7. Expression of *OPA1* protein in fibroblasts from the OPA1_R932C patient and from controls. Cellular extracts were analyzed by western blotting using antibodies against *OPA1* and HSP60 as described in materials and methods. HSP60 was used as a mitochondrial marker and as a control for protein loading.

onset presentation. This finding, taken together with several recently published observations, demonstrates that the clinical spectrum of OPA1-associated optic neuropathies is much larger than previously believed. The systematic search for *OPA1* mutations should therefore prove useful in unexplained and atypical cases of optic atrophy.

ACKNOWLEDGMENTS

We are grateful to Kanaya Malkani for critical reading and comments on the manuscript. This work was supported by INSERM, the University Hospital of Angers (PHRC 04–12), the University of Angers, and by grants from the following associations of patients: Association contre les Maladies Mitochondriales (AMMi), Retina France, Ouvrir les Yeux (OLY), and Union Nationale des Aveugles et Déficiants Visuels (UNADEV).

REFERENCES

- Johnston PB, Gaster RN, Smith VC, Tripathi RC. A clinicopathological study of autosomal dominant optic atrophy. *Am J Ophthalmol* 1979; 88:868-75. [PMID: 315716]
- Hoyt CS. Autosomal dominant optic atrophy: a spectrum of disability. *Ophthalmology* 1980; 87:245-51. [PMID: 7422264]
- Lyle WM. Genetic risks. Waterloo, Ontario: Univ of Waterloo Press;1990.
- Kjer B, Eiberg H, Kjer P, Rosenberg T. Dominant optic atrophy mapped to chromosome 3q region II. Clinical and epidemiological aspects. *Acta Ophthalmol Scand* 1996; 74:3-7. [PMID: 8689476]
- Votruba M, Fitzke FW, Holder GE, Carter A, Bhattacharya SS, Moore AT. Clinical features in affected individuals from 21 pedigrees with dominant optic atrophy. *Arch Ophthalmol* 1998; 116:351-8. [PMID: 9514489]
- Kjer P, Jensen OA, Klinken L. Histopathology of eye, optic nerve and brain in a case of dominant optic atrophy. *Acta Ophthalmol (Copenh)* 1983; 61:300-12. [PMID: 6880639]
- Alexander C, Votruba M, Pesch UE, Thiselton DL, Mayer S, Moore A, Rodriguez M, Kellner U, Leo-Kottler B, Auburger G, Bhattacharya SS, Wissinger B. *OPA1*, encoding a dynamin related GTPase, is mutated in autosomal dominant optic atrophy linked to chromosome 3q28. *Nat Genet* 2000; 26:211-5. [PMID: 11017080]
- Delettre C, Lenaers G, Griffoin JM, Gigarel N, Lorenzo C, Belenguer P, Pelloquin L, Grosgeorge J, Turc-Carel C, Perret E, Astarie-Dequeker C, Lasquellec L, Arnaud B, Ducommun B, Kaplan J, Hamel CP. Nuclear gene *OPA1*, encoding a mitochondrial dynamin-related protein, is mutated in dominant optic atrophy. *Nat Genet* 2000; 26:207-10. [PMID: 11017079]
- Delettre C, Griffoin JM, Kaplan J, Dollfus H, Lorenz B, Faivre L, Lenaers G, Belenguer P, Hamel CP. Mutation spectrum and splicing variants in the *OPA1* gene. *Hum Genet* 2001; 109:584-91. [PMID: 11810270]
- Ferre M, Amati-Bonneau P, Tourmen Y, Malthiery Y, Reynier P. eOPA1: An online database for *OPA1* mutations. *Hum Mutat* 2005; 25:423-8. [PMID: 15832306]
- Olichon A, Emorine LJ, Descoins E, Pelloquin L, Brichese L, Gas N, Guillou E, Delettre C, Valette A, Hamel CP, Ducommun B, Lenaers G, Belenguer P. The human dynamin-related protein *OPA1* is anchored to the mitochondrial inner membrane facing the inter-membrane space. *FEBS Lett* 2002; 523:171-6. [PMID: 12123827]
- Olichon A, Baricault L, Gas N, Guillou E, Valette A, Belenguer P, Lenaers G. Loss of *OPA1* perturbs the mitochondrial inner membrane structure and integrity, leading to cytochrome c release and apoptosis. *J Biol Chem* 2003; 278:7743-6. [PMID: 12509422]
- Frezza C, Cipolat S, Martins de Brito O, Micaroni M, Beznoussenko GV, Rudka T, Bartoli D, Polishuck RS, Danial NN, De Strooper B, Scorrano L. *OPA1* controls apoptotic cristae remodeling independently from mitochondrial fusion. *Cell* 2006; 126:177-89. [PMID: 16839885]
- Hudson G, Amati-Bonneau P, Blakely EL, Stewart JD, He L, Schaefer AM, Griffiths PG, Ahlqvist K, Suomalainen A, Reynier P, McFarland R, Turnbull DM, Chinnery PF, Taylor RW. Mutation of *OPA1* causes dominant optic atrophy with external ophthalmoplegia, ataxia, deafness and multiple mitochondrial DNA deletions: a novel disorder of mtDNA maintenance. *Brain* 2008; 131:329-37. [PMID: 18065439]
- Amati-Bonneau P, Valentino ML, Reynier P, Gallardo ME, Bornstein B, Boissière A, Campos Y, Rivera H, de la Aleja JG, Carroccia R, Iommarini L, Labauge P, Figarella-Branger D, Marcorelles P, Furby A, Beauvais K, Letourmel F, Liguori R, La Morgia C, Montagna P, Liguori M, Zanna C, Rugolo M, Cossarizza A, Wissinger B, Verny C, Schwarzenbacher R, Martin MA, Arenas J, Ayuso C, Garesse R, Lenaers G, Bonneau D, Carelli V. *OPA1* mutations induce mitochondrial DNA instability and optic atrophy 'plus' phenotypes. *Brain* 2008; 131:338-51. [PMID: 18158317]
- Baris O, Delettre C, Amati-Bonneau P, Surget MO, Charlin JF, Catier A, Derieux L, Guyomard JL, Dollfus H, Jonveaux P, Ayuso C, Maumenee I, Lorenz B, Mohammed S, Tourmen Y, Bonneau D, Malthiery Y, Hamel C, Reynier P. Fourteen novel *OPA1* mutations in Autosomal Dominant Optic Atrophy including two de novo mutations in sporadic optic atrophy. *Hum Mutat* 2003; 21:656. [PMID: 14961560]
- Cornille K, Milea D, Amati-Bonneau P, Procaccio V, Zazoun L, Guillet V, El Achouri G, Delettre C, Gueguen N, Loiseau D, Muller A, Ferré M, Chevrollier A, Wallace DC, Bonneau D, Hamel C, Reynier P, Lenaers G. Reversible optic neuropathy with *OPA1* exon 5b mutation. *Ann Neurol* 2008; 63:667-71. [PMID: 18360822]
- Amati-Bonneau P, Guichet A, Olichon A, Chevrollier A, Viala F, Miot S, Ayuso C, Odent S, Arrouet C, Verny C, Calmels MN, Simard G, Belenguer P, Wang J, Puel JL, Hamel C, Malthiery Y, Bonneau D, Lenaers G, Reynier P. *OPA1* R445H mutation in optic atrophy associated with sensorineural deafness. *Ann Neurol* 2005; 58:958-63. [PMID: 16240368]
- Spinazzi M, Cazzola S, Bortolozzi M, Baracca A, Loro E, Casarin A, Solaini G, Sgarbi G, Casalena G, Cenacchi G, Malena A, Frezza C, Carrara F, Angelini C, Scorrano L, Salviati L, Vergani L. A novel deletion in the GTPase domain of *OPA1* causes defects in mitochondrial morphology and distribution, but not in function. *Hum Mol Genet* 2008; 17:3291-302. [PMID: 18678599]
- Payne M, Yang Z, Katz BJ, Warner JE, Weight CJ, Zhao Y, Pearson ED, Treft RL, Hillman T, Kennedy RJ, Meire FM,

- Zhang K. Dominant optic atrophy, sensorineural hearing loss, ptosis, and ophthalmoplegia: A syndrome caused by a missense mutation in OPA1. *Am J Ophthalmol* 2004; 138:749-55. [PMID: 15531309]
21. Lodi R, Tonon C, Valentino ML, Iotti S, Clementi V, Malucelli E, Barboni P, Longanesi L, Schimpf S, Wissinger B, Baruzzi A, Barbiroli B, Carelli V. Deficit of in vivo mitochondrial ATP production in OPA1-related dominant optic atrophy. *Ann Neurol* 2004; 56:719-23. [PMID: 15505825]
 22. Chevrollier A, Guillet V, Loiseau D, Gueguen N, de Crescenzo MA, Verny C, Ferre M, Dollfus H, Odent S, Milea D, Goizet C, Amati-Bonneau P, Procaccio V, Bonneau D, Reynier P. Hereditary optic neuropathies share a common mitochondrial coupling defect. *Ann Neurol* 2008; 63:794-8. [PMID: 18496845]
 23. Olichon A, Landes T, Arnauné-Pelloquin L, Emorine LJ, Mils V, Guichet A, Delettre C, Hamel C, Amati-Bonneau P, Bonneau D, Reynier P, Lenaers G, Belenguer P. Effects of OPA1 mutations on mitochondrial morphology and apoptosis: relevance to ADOA pathogenesis. *J Cell Physiol* 2007; 211:423-30. [PMID: 17167772]
 24. Loiseau D, Chevrollier A, Verny C, Guillet V, Gueguen N, Pou de Crescenzo MA, Ferré M, Malinge MC, Guichet A, Nicolas G, Amati-Bonneau P, Malthiery Y, Bonneau D, Reynier P. Mitochondrial coupling defect in Charcot-Marie-Tooth type 2A disease. *Ann Neurol* 2007; 61:315-23. [PMID: 17444508]
 25. Rustin P, Chretien D, Bourgeron T, Gerard B, Rotig A, Saudubray JM, Munnich A. Biochemical and molecular investigations in respiratory chain deficiencies. *Clin Chim Acta* 1994; 228:35-51. [PMID: 7955428]
 26. Cassereau J, Chevrollier A, Gueguen N, Malinge MC, Letournel F, Nicolas G, Richard L, Ferre M, Verny C, Dubas F, Procaccio V, Amati-Bonneau P, Bonneau D, Reynier P. Mitochondrial complex I deficiency in GDAP1-related autosomal dominant Charcot-Marie-Tooth disease (CMT2K). *Neurogenetics*. 2008 [PMID: 19089472]
 27. Andrews RM, Kubacka I, Chinnery PF, Lightowlers RN, Turnbull DM, Howell N. Reanalysis and revision of the Cambridge reference sequence for human mitochondrial DNA. *Nat Genet* 1999; 23:147. [PMID: 10508508]
 28. Votruba M, Moore AT, Bhattacharya SS. Clinical features, molecular genetics and pathophysiology of dominant optic atrophy. *J Med Genet* 1998; 35:793-800. [PMID: 9783700]
 29. Cohn AC, Toomes C, Potter C, Towns KV, Hewitt AW, Inglehearn CF, Craig JE, Mackey DA. Autosomal dominant optic atrophy: penetrance and expressivity in patients with OPA1 mutations. *Am J Ophthalmol* 2007; 143:656-62. [PMID: 17306754]
 30. Misaka T, Miyashita T, Kubo Y. Primary structure of a dynamin-related mouse mitochondrial GTPase and its distribution in brain, subcellular localization, and effect on mitochondrial morphology. *J Biol Chem* 2002; 277:15834-42. [PMID: 11847212]
 31. Chen AS, Kovach MJ, Herman K, Avakian A, Frank W, Forrester S, Lin JP, Kimonis V. Clinical heterogeneity in autosomal dominant optic atrophy in two 3q28-qter linked central Illinois families. *Genet Med* 2000; 2:283-9. [PMID: 11399209]
 32. Roggeveen HC, de Winter AP, Went LN. Studies in dominant optic atrophy. *Ophthalmic Paediatr Genet* 1985; 5:103-9. [PMID: 4058864]
 33. Payne M, Yang Z, Katz BJ, Warner JE, Weight CJ, Zhao Y, Pearson ED, Treft RL, Hillman T, Kennedy RJ, Meire FM, Zhang K. Dominant optic atrophy, sensorineural hearing loss, ptosis, and ophthalmoplegia: a syndrome caused by a missense mutation in OPA1. *Am J Ophthalmol* 2004; 138:749-55. [PMID: 15531309]
 34. Puomila A, Huoponen K, Mäntyjärvi M, Hämäläinen P, Paananen R, Sankila EM, Savontaus ML, Somer M, Nikoskelainen E. Dominant optic atrophy: correlation between clinical and molecular genetic studies. *Acta Ophthalmol Scand* 2005; 83:337-46. [PMID: 15948788]
 35. Han J, Thompson-Lowrey AJ, Reiss A, Mayorov V, Jia H, Biousse V, Newman NJ, Brown MD. OPA1 mutations and mitochondrial DNA haplotypes in autosomal dominant optic atrophy. *Genet Med* 2006; 8:217-25. [PMID: 16617242]
 36. Carelli V, La Morgia C, Iommarini L, Carroccia R, Mattiazzi M, Sangiorgi S, Farne' S, Maresca A, Foscari B, Lanzi L, Amadori M, Bellan M, Valentino ML. Mitochondrial optic neuropathies: how two genomes may kill the same cell type? *Biosci Rep* 2007; 27:173-84. [PMID: 17479363]

Appendix 1. Amplification and sequencing primers for OPA1 gene.

The nucleotide sequence of the primers used to amplify and sequence the 30 OPA1 coding exons, including exon-intron junctions, is given according to the GenBank reference

sequence NC_000003.10. To access the data, click or select the words “[Appendix 1](#).” This will initiate the download of a pdf file that contains the information.

Appendix 2. Amplification and sequencing primers for mtDNA.

The nucleotide sequence of the primers used to amplify and sequence the entire mitochondrial DNA is given according the Revised Cambridge Reference Sequence of the Human Mitochondrial DNA (RefSeq: AC_000021.2)

numbering, described as being the “Light strand.” Primers in *Italic* were those used for DNA amplification. To access the data, click or select the words “[Appendix 2](#).” This will initiate the download of a pdf file that contains the information.

Appendix 3. Representative deconvolved images used to quantify mitochondrial length:

Mitochondrial length was determined using integrated morphometric analysis of the Mitotracker®-labeled regions created after deconvolution. The Figure shows examples of the mitochondrial network observed in the patient's

fibroblasts. To access the data, click or select the words “[Appendix 3](#).” This will initiate the download of a pdf file that contains the information.